THE MODWT ANALYSIS OF THE RELATIONSHIP BETWEEN MORTALITY AND AMBIENT TEMPERATURE FOR PRAGUE, CZECH REPUBLIC

Milan Bašta*

1. Introduction and data

In this paper, we use the maximum overlap discrete wavelet transform to study the relationship between the average ambient temperature (T) and the number of deaths (D) due to cardiovascular diseases. The purpose of the use of the wavelet transform is to study the relationships in separate frequency bands. Such an approach is intriguing as it might enable us to reveal relationships that might otherwise remain undetected when explored by „classical" methods.

We use daily data for Prague, Czech Republic, during the period from January 1, 2000, to December 31, 2008. The data were provided by the Czech Statistical Office (http://www.czso.cz/) and the Czech Hydrometeorological Institute (http://www.chmi.cz/). The respective time series are plotted in Figure 1.

As has been already demonstrated in a vast amount of literature, ambient temperature impacts the numbers of deaths considerably. There are several well-known aspects of this relationship. For example, in Figure 2 we plot D against T and smooth the scatterplot with the lowess smoother[1]. The plot slightly suggests the well-known V-shaped relationship between T and D with winter (i.e. low) temperatures accompanied on average by a higher number of deaths and spring and summer (i.e. high) temperatures accompanied on average by a lower number of deaths. The minimum number of deaths occurs close to 16°C. The seasonal relationship between T and D does not appear to be strong from Figure 2, since it is "buried" in the short-term dynamics. Later in the text, we show that when adjustment is made for these short-term dynamics the seasonal relationship is indeed strong.

The antiphase relationship in the seasonal dynamics of D and T – just revealed in Figure 2 for our data – has been identified among others by Laschewski & Jendritzky

* University of Economics, Prague, Faculty of Informatics and Statistics (milan.basta@vse.cz).

This paper was written with the support of the Grant Agency of the Czech Republic No. 402/09/0369, Modeling of Demographic Time Series in the Czech Republic.

We acknowledge the support of the Grant Agency of the Czech Republic No. 402/09/0369, Modeling of Demographic Time Series in the Czech Republic. We acknowledge the use of data provided by the Czech Statistical Office and the Czech Hydrometeorological Institute.

1 The lowess smoothing is a method of smoothing the data in a scatterplot based on the locally weighted polynomial regression (Cleveland, 1979). We will apply the approach of the lowess smoothing in this text very often, in order to roughly describe and see the "average" relationships in the data.

(2002), who use data for SW Germany during the period 1968-1997 and show that mortality peaks in February and has its minimum in August. A similar V-shaped pattern for cardiovascular mortality against temperature was also identified by Huynen et al. (2001), who use data for Netherlands during 1979-1997. Recently, Bašta et al. (2010) have confirmed this seasonal type of relationship between T and D for Prague, Czech Republic, during the period 2000-2008.

Figure 1

The daily time series of the average temperature (top) and the daily time series of the number of deaths (bottom). The ticks on the *x* axis separate individual calendar years (2000–2008).

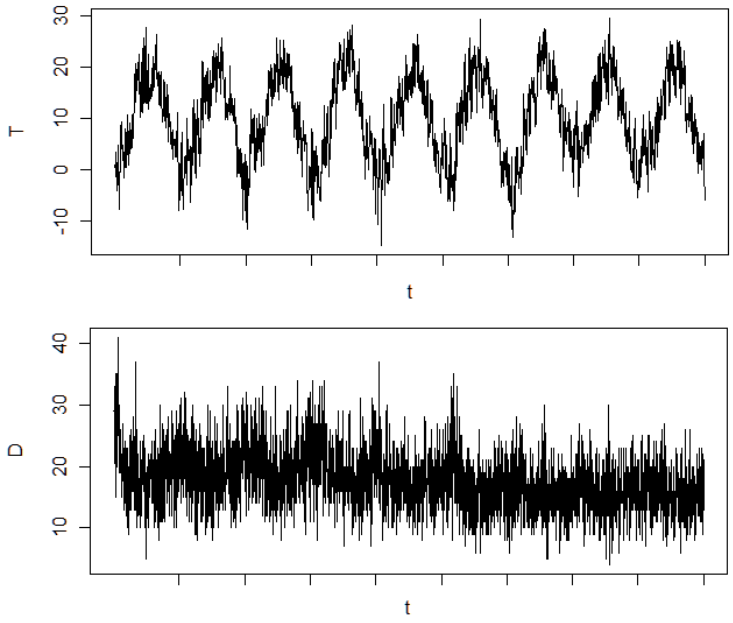

Another well-known fact about the relationship between ambient temperature and mortality is that extremely hot events in summer cause an increase in the numbers of deaths. For example, Rooney et al. (1998) report that severely high temperatures in July and August 1995 in England and Wales increased mortality significantly. The authors report that people with respiratory and cerebrovascular diseases were affected most noticeably. Laschewski & Jendritzky (2002) show that pronounced heat loads during the summer mortality minimum cause sharp increases in mortality. An increase in mortality during heat waves was also confirmed by Huynen et al. (2001). They report that old people and those suffering from respiratory diseases were affected the most. Similarly, Grize et al. (2003) report that an all-case increase in mortality occurred in Switzerland during the heat waves in summer 2003. Again, elderly people were affected profoundly.

Not only heat waves but also cold spells affect the numbers of deaths. For example, Díaz et al. (2005) explore the effect of extremely cold weather on the mortality of elderly people in Madrid during the period 1986–1997 and report an impact (lagged by

several days) of cold weather on the mortality from respiratory and circulatory diseases. Similarly, Keatinge & Donaldson (1995), studying British data, report that cold spells in winter cause an increase in mortality due to ischemic heart disease. Larsen (1990) studied temperature-related mortality for the United Stated from 1921 to 1985 using the data for six US states. She reports that unusually cold temperatures in winter, spring and autumn months cause higher mortality.

In our paper, we suggest the existence of a relationship between changes in weekly average temperatures and changes in weekly average number of deaths for summer months. For this purpose, we use the maximum overlap discrete wavelet transform, which will be briefly introduced in the next section.

Figure 2

The lowess smoothing of the scatterplot of *D* against *T* showing the V-shaped relationship between *T* and *D*.

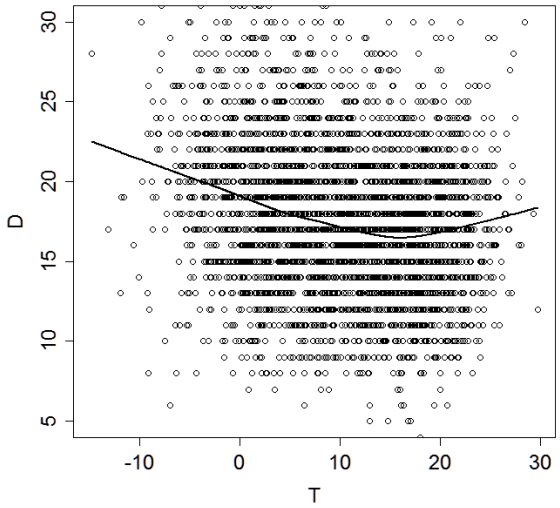

2. Maximum overlap discrete wavelet transform

The maximum overlap discrete wavelet transform (MODWT) will be summarized in this section. Our summary of MODWT is based on Percival & Walden (2002) and Bašta (2010), which encompass details and proofs of the statements given below. Further books may be recommended too – e.g. Vidakovic (1999) gives a more technical and abstract introduction to wavelets. Gencay, Selcuk & Whitcher (2002) present a less technical introduction with applications in finance and economics. At first, linear filtration will be introduced; afterwards, wavelet and scaling filters and MODWT wavelet and scaling coefficients will be defined and their properties discussed.

Linear filtration

Let the finite sequence $\{a_t : t = 0, ..., M - 1\}$ of real-valued (non-random) variables be called the linear filter of the length M. For the ease of notation, we will use the notation $\{a_t\}$ whenever the values that t can assume are clear from the text. Let the linear

filtration of the discrete-time stationary stochastic process $\{X_t: t = ...,-1,0,1, ...\}$ with the linear filter $\{a_t\}$ be a discrete-time stationary stochastic process $\{Y_t: t = ...,-1,0,1, ...\}$ defined as [2]

$$Y_t \equiv \sum_{m=0}^{M-1} a_m X_{t-m}, \quad \text{for } t = ..., -1, 0, 1, ... \ .$$

Let $S_X(.)$ and $S_Y(.)$ be the spectrum of the process $\{X_t\}$ and the process $\{Y_t\}$ defined as

$$S_X(f) \equiv \sum_{\tau=-\infty}^{\infty} \gamma_{X,\tau} \exp(-\mathrm{i}2\pi f \tau), \quad \text{for } f \in R,$$

$$S_Y(f) \equiv \sum_{\tau=-\infty}^{\infty} \gamma_{Y,\tau} \exp(-\mathrm{i}2\pi f \tau), \quad \text{for } f \in \mathrm{R},$$

where i is the imaginary unit and f is a real-valued parameter called the frequency and the sequences $\{\gamma_{X,\tau}: \tau = ...,-1,0,1, ...\}$ and $\{\gamma_{Y,\tau}: \tau = ...,-1,0,1, ...\}$ are the autocovariance sequences of the processes $\{X_t\}$ and $\{Y_t\}$. Since the spectrum is an even and periodic function of frequency, with the period equal to unity, further on it is sufficient to study and explore spectra only in the range of frequencies [0, 1/2]. We may informally say that the spectra $S_X(.)$ and $S_Y(.)$ inform us about the "frequency content" of the stochastic processes $\{X_t\}$ and $\{Y_t\}$. The higher the spectrum in a given frequency interval, the larger the contribution of the "dynamics" of that frequency interval to the variance of the process. More specifically, it can be shown that

$$\gamma_{X,0} = 2 \int_0^{+1/2} S_X(f)\, df, \qquad \gamma_{Y,0} = 2 \int_0^{+1/2} S_Y(f)\, df.$$

The effect of the linear filtration with the linear filter $\{a_t\}$ of the stochastic process $\{X_t\}$ is given by the characteristics of the linear filter $\{a_t\}$. An important characteristics is the frequency response $F_a(.)$ of this filter defined as the Fourier transform of $\{a_t\}$, i.e.

$$F_a(f) \equiv \sum_{t=0}^{M-1} a_t \exp(-\mathrm{i}2\pi f t), \quad \text{for } f \in R.$$

The function $|F_a(.)|^2$, i.e. the square of the modulus of $F_a(.)$, is called the squared gain function of the filter $\{a_t\}$. The squared gain function is an even and periodic function of frequency, with the period equal to unity. Therefore, further on it is sufficient to explore it only in the frequency range [0, 1/2]. The squared gain function informs us about frequencies that are passed and about frequencies that are attenuated by the effect of the linear filtration. More specifically, it can be shown that

$$S_Y(f) = \left|F_a(f)\right|^2 S_X(f), \quad \text{for } 0 \le f \le 1/2. \tag{1}$$

2 Again, shorthand notations $\{X_t\}$, $\{Y_t\}$ etc. might be used instead of $\{X_t: t = ...,-1,0,1,...\}$, $\{Y_t: t = ...,-1,0,1,...\}$ etc. whenever the values that t can assume are clear from the text.

Wavelet and scaling filters

To introduce MODWT, we need to define a special set of linear filters at first. This special set may be created with the knowledge of two elementary linear filters: the filter $\{h_{1,t}: t = 0, \ldots, L_1 - 1\}$ and the filter $\{g_{1,t}: t = 0,\ldots, L_1 - 1\}$, both of lengths L_1. The linear filters $\{h_{1,t}\}$ and $\{g_{1,t}\}$ are interconnected via the so-called quadrature mirror relationship, i.e.

$$g_{1,t} \equiv (-1)^{t+1} h_{1,L_1-1-t}$$

and fulfill certain specific conditions, e.g.,

$$\sum_{t=0}^{L_1-1} h_{1,t} = 0, \quad \sum_{t=0}^{L_1-1} h_{1,t}^2 = \frac{1}{2}, \quad \sum_{t=0}^{L_1-1} h_{1,t} h_{1,t+2n} = 0, \text{ for any nonzero integer } n,$$

$$\sum_{t=0}^{L_1-1} g_{1,t} = 1, \quad \sum_{t=0}^{L_1-1} g_{1,t}^2 = \frac{1}{2} \quad \sum_{t=0}^{L_1-1} g_{1,t} g_{1,t+2n} = 0, \text{ for any nonzero integer } n.$$

In Figure 3, various pairs of filters $\{h_{1,t}\}$ and $\{g_{1,t}\}$ are presented, corresponding to various so-called families of wavelets.

An ideal filter with the nominal pass band $[d, u]$, where d and u are real parameters satisfying $0 \le d \le u \le 1/2$, is such a filter whose squared gain function is given as

$$\left|F_{ideal}^{d,u}(f)\right|^2 \equiv \begin{cases} 1, & \text{for } d \le f \le u \\ 0, & \text{for } 0 \le f < d \text{ and for } u < f \le 1/2. \end{cases}$$

In Figure 4, the squared gain functions are presented for filters of Figure 3. It can be intuitively seen that $\{h_{1,t}\}$ is approximately an ideal filter with the nominal pass band [1/4, 1/2]. On the other hand, $\{g_{1,t}\}$ is approximately an ideal low-pass[3] filter with the nominal pass band [0, 1/4].

For a given pair of filters $\{h_{1,t}\}$ and $\{g_{1,t}\}$, two *sets* of filters may be created via the so-called pyramid algorithm. This algorithm will not be specified here, because it is technical and will be of no use for the purpose of this text (details on the algorithm can be found, e.g. in Percival & Walden, 2002; Gencay, Selcuk & Whitcher, 2002; Vidakovic, 1999; Bašta, 2010). Only the properties of the filters from both sets will be discussed in this text.

First, let us call the filters from the first set the *wavelet* filters and let us denote them as follows: $\{h_{1,t}: t = 0, \ldots, L_1 - 1\}$, $\{h_{2,t}: t = 0, \ldots, L_2 - 1\}$, $\{h_{3,t}: t = 0, \ldots, L_3 - 1\}$, etc., where the filter $\{h_{1,t}: t = 0, \ldots, L_1 - 1\}$ is the filter that has been defined already above, and where L_1, L_2, L_3 are the lengths of these filters. The word "etc." in the previous sentence is to mean that the set of the wavelet filters is infinite. The wavelet filters are indexed by positive integers and generally, the jth wavelet filter of the set is denoted as $\{h_{j,t}: t = 0, \ldots, L_j - 1\}$ and has the length $L_j = (2^j - 1)(L_1 - 1) + 1$.

Similarly, let us call the filters from the second set the *scaling* filters and let us denote them as follows: $\{g_{1,t}: t = 0, \ldots, L_1 - 1\}$, $\{g_{2,t}: t = 0, \ldots, L_2 - 1\}$, $\{g_{3,t}: t = 0, \ldots,$

3 The term low-pass stems from the fact that this filter passes low frequencies and attenuates high frequencies.

$L_3 - 1\}$, etc., where the filter $\{g_{1,t}: t = 0, \ldots, L_1 - 1\}$ is the filter already defined in the previous paragraphs, and where L_1, L_2, L_3 are the lengths of these filters. Again, the set of the scaling filters is infinite and generally, the jth filter of the set is denoted as $\{g_{j,t}: t = 0, \ldots, L_j - 1\}$ and has the length $L_j = (2^j - 1)(L_1 - 1) + 1$.

It is important to stress that the filter $\{h_{j,t}\}$ (for $j = 1,2,...$) is approximately an ideal filter with the nominal pass band $[2^{-(j+1)}, 2^{-j}]$ and $\{g_{j,t}\}$ (for $j = 1,2,...$) is approximately an ideal low-pass filter with the nominal pass band $[0, 2^{-(j+1)}]$. To illustrate, let us present one example of wavelet and scaling filters: the filters based on the so-called Haar family. For the Haar wavelet filter $\{h_{j,t}: t = 0,..., L_j - 1\}$ (for $j = 1,2,...$), we can write

$$h_{j,t} \equiv \begin{cases} \dfrac{1}{2^j}, & \text{for } t = 0,...,2^{j-1} - 1 \\ -\dfrac{1}{2^j}, & \text{for } t = 2^{j-1},...,2^j - 1 \end{cases}$$

and for the Haar scaling filters $\{g_{j,t}: t = 0,..., L_j - 1\}$ (for $j = 1,2,...$), we can write

$$g_{j,t} \equiv \frac{1}{2^j}, \quad \text{for } t = 0,...,2^j - 1 \ .$$

Thus, the lengths of the Haar filters $\{h_{j,t}\}$ and $\{g_{j,t}\}$ (for $j = 1,2, ...$) are equal to $L_j = 2^j$. The Haar MODWT wavelets and Haar MODWT scaling filters are plotted in Figure 5. In Figure 6, we present the squared gain functions for the Haar filters of Figure 5. We can intuitively see that the Haar wavelet filter $\{h_{j,t}\}$ is approximately an ideal filter with the nominal pass band $[2^{-(j+1)}, 2^{-j}]$ and the Haar scaling filter $\{g_{j,t}\}$ is approximately an ideal low-pass filter with the nominal pass band $[0, 2^{-(j+1)}]$.

Figure 3

Pairs of linear filters $\{h_{1,t}\}$ (in the top row) and $\{g_{1,t}\}$ (in the bottom row) are presented in each column. The first column (i.e. the first pair) corresponds to the family of Haar filters, the second column to the family of Daubechies-4 filters, the third column to the family of Daubechies-6 filters, and the fourth column to the family of Daubechies-8 filters.

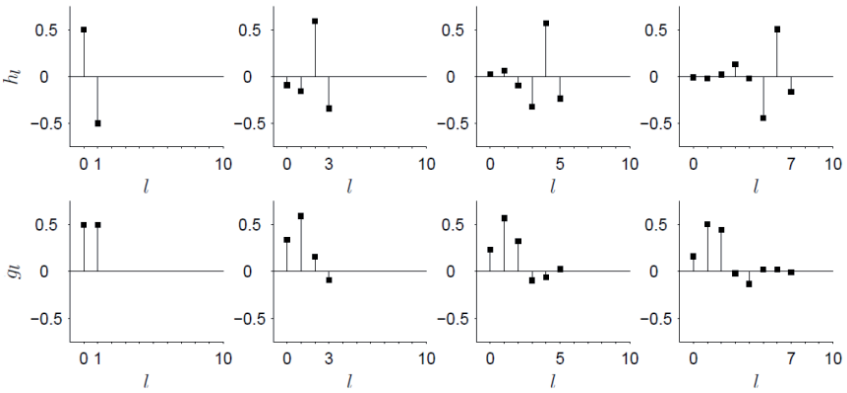

Figure 4

Squared gain functions are given for the filters of Figure 3, i.e. the top row corresponds to the squared gain function of the (from left to right) Haar, Daubechies-4, Daubechies-6 and Daubechies-8 $\{h_{1,t}\}$ filter. Similarly, the bottom row corresponds to the squared gain function of the (from left to right) Haar, Daubechies-4, Daubechies-6 and Daubechies-8 $\{g_{1,t}\}$ filter. The dotted rectangles depict the squared gain functions of ideal filters.

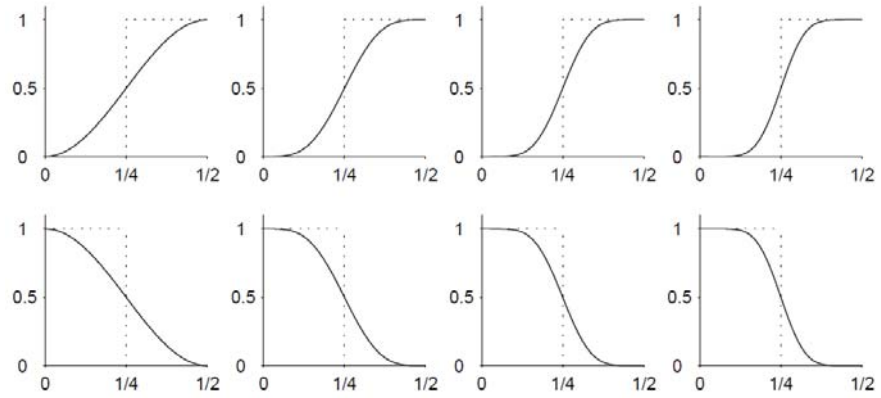

Figure 5

Top row: the Haar MODWT wavelet filters $\{h_{1,t}\}$, $\{h_{2,t}\}$, $\{h_{3,t}\}$ and $\{h_{4,t}\}$. Bottom row: the Haar MODWT scaling filters $\{g_{1,t}\}$ $\{g_{2,t}\}$, $\{g_{3,t}\}$ and $\{g_{4,t}\}$.

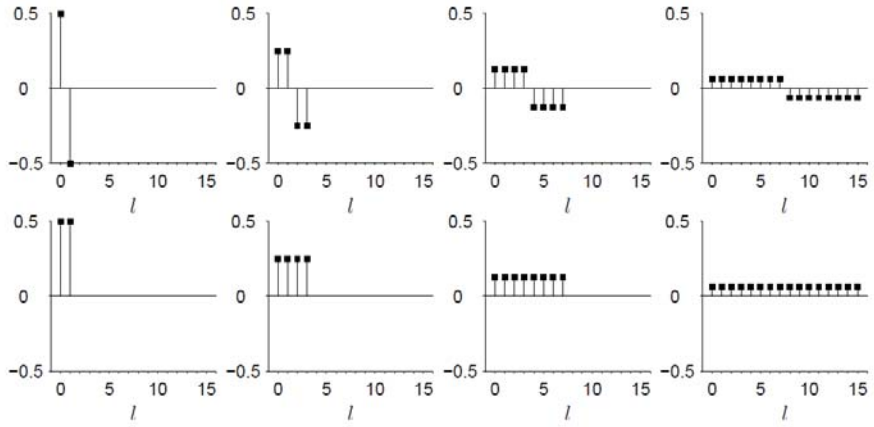

Figure 6

The squared gain functions of the Haar MODWT wavelet filters $\{h_{1,t}\}$, $\{h_{2,t}\}$, $\{h_{3,t}\}$ and $\{h_{4,t}\}$ (top row) and of the Haar MODWT scaling filters $\{g_{1,t}\}$, $\{g_{2,t}\}$, $\{g_{3,t}\}$ and $\{g_{4,t}\}$ (bottom row). The squared gain functions of the respective ideal filters are shown as rectangles.

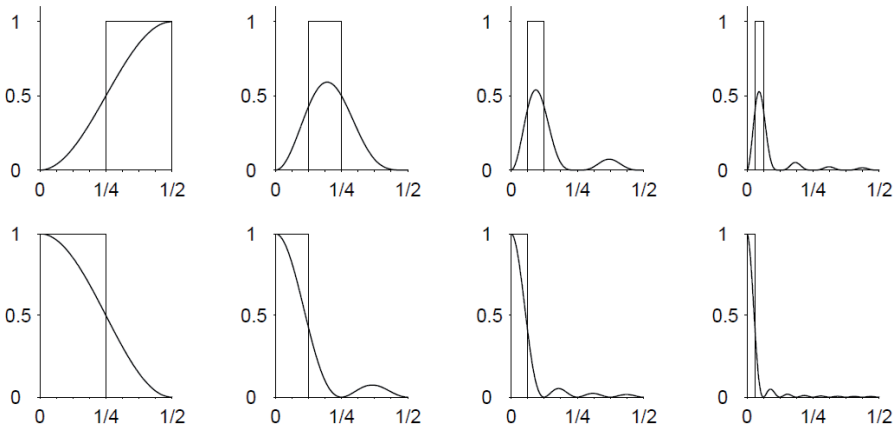

MODWT coefficients

Let $\{X_t: t = 0, 1, ..., N-1\}$ be a discrete-time stationary stochastic process. For $j = 1, 2, ...$ let us define a discrete-time stochastic process $\{W_{j,t}: t = 0, 1, ..., N-1\}$ and a discrete-time stochastic process $\{V_{j,t}: t = 0, 1, ..., N-1\}$ as

$$W_{j,t} \equiv \sum_{m=0}^{L_j-1} h_{j,m} X_{(t-m) \bmod N}, \quad \text{for} \quad t = 0,...,N-1 \tag{2}$$

$$V_{j,t} \equiv \sum_{m=0}^{L_j-1} g_{j,m} X_{(t-m) \bmod N}, \quad \text{for} \quad t = 0,...,N-1 \tag{3}$$

where mod denotes the operation modulo. The process $\{W_{j,t}\}$ is called the jth level MODWT wavelet coefficients and the process $\{V_{j,t}\}$ is called the jth level MODWT scaling coefficients. The modulo operation affects the construction of $W_{j,t}$ and $V_{j,t}$ for $0 \le t < L_j - 1$. On the other hand, the construction of $W_{j,t}$ and $V_{j,t}$ for $L_j - 1 \le t \le N-1$ would remain unaffected if the modulo operation was left out in Equation 2 and Equation 3. Thus, we say that $W_{j,t}$ and $V_{j,t}$ for $0 \le t < L_j - 1$ are affected by the circularity assumption, whereas $W_{j,t}$ and $V_{j,t}$ for $L_j - 1 \le t \le N-1$ are not.

Since the stochastic process $\{X_t\}$ is stationary, it can be shown (see, e.g. Percival & Walden, 2002; or Bašta, 2010) that $\{W_{j,t}: t = 0, 1, ..., N-1\}$ and $\{V_{j,t}: t = 0, 1, ..., N-1\}$ (for $j = 1,2, ...$) are stationary too and that

$$E(W_{j,t}) = 0, \quad \text{for} \quad t = L_j - 1,...,N-1.$$

Since the *j*th level wavelet coefficients $\{W_{j,t}\}$ have been obtained with the use of the linear filter $\{h_{j,t}\}$ – which is approximately an ideal filter with the nominal pass band $[2^{-(j+1)}, 2^{-j}]$, it is intuitively clear that the *j*th level wavelet coefficients are associated with the same frequency range and capture the dynamics of the stochastic process $\{X_t\}$ in this frequency range. It can also be shown (see Percival & Walden, 2002) that the *j*th level wavelet coefficients $\{W_{j,t}\}$ are for many families of wavelets associated with changes between two adjacent weighted averages whereas these weighted averages have an effective length of 2^{j-1}.

Similarly, *j*th level scaling coefficients $\{V_{j,t}\}$ have been obtained with the use of the linear filter $\{g_{j,t}\}$, which is approximately an ideal low-pass filter for the frequency range $[0, 2^{-(j+1)}]$. Thus, it is intuitively clear that the *j*th level scaling coefficients are associated with the same frequency range and capture long-term dynamics of the stochastic process $\{X_t\}$ (since low frequencies correspond to high periods and thus trending motions).

3. The MODWT analysis of temperature and numbers of deaths

Now, let $\{T_t: t = 0, ..., N-1\}$ be an observed time series representing the daily average temperature in Prague, Czech Republic, during the period from January 1, 2000, to December 31, 2008 (see also Figure 1). The positive integer N is the length of the time series. A shorthand notation T may be used to denote this time series. Analogously, let $\{D_t: t = 0, ..., N-1\}$ be the observed time series of the daily number of deaths due to cardiovascular diseases in Prague, Czech Republic, during the period from January 1, 2000, to December 31, 2008 (see also Figure 1). A shorthand notation D may be used to denote this time series.

The MODWT analysis of $\{T_t: t = 0, ..., N-1\}$ as well as $\{D_t: t = 0, ..., N-1\}$ has been carried out, i.e. series of wavelet and scaling coefficients for levels $j = 1, 2, ..., 10$ have been calculated in the sense of Equation 2 and Equation 3. Haar filters have been used. We will denote the resultant series of wavelet and scaling coefficient as follows:

- let $\{T.wav1_t: t = 0, ..., N-1\}$, $\{T.wav2_t: t = 0, ..., N-1\}$, ..., $\{T.wav10_t: t = 0, ..., N-1\}$ be the series of wavelet coefficients of levels $j = 1,2, ..., 10$ for T. The shorthand notation *T.wav1*, *T.wav2*, ... , *T.wav10* may be used.
- let $\{T.sca1_t: t = 0, ..., N-1\}$, $\{T.sca2_t: t = 0, ..., N-1\}$, ..., $\{T.sca10_t: t = 0, ..., N-1\}$ be the series of scaling coefficients of levels $j = 1,2, ..., 10$ for T. The shorthand notation *T.sca1*, *T.sca2*, ... , *T.sca10* may be used.
- let $\{D.wav1_t: t = 0, ..., N-1\}$, $\{D.wav2_t: t = 0, ..., N-1\}$, ..., $\{D.wav10_t: t = 0, ..., N-1\}$ be the series of wavelet coefficients of levels $j = 1,2, ..., 10$ for D. The shorthand notation *D.wav1*, *D.wav2*, ... , *D.wav10* may be used.
- let $\{D.sca1_t: t = 0, ..., N-1\}$, $\{D.sca2_t: t = 0, ..., N-1\}$, ..., $\{D.sca10_t: t = 0, ..., N-1\}$ be the series of scaling coefficients of levels $j = 1,2, ..., 10$ for D. The shorthand notation *D.sca1*, *D.sca2*, ... , *D.sca10* may be used.

A part of the results is depicted in Figure 7 for T and in Figure 8 for D – more specifically, series *T.wav2*, *T.wav4*, *T.wav6*, *T.wav8* and *T.sca10* are plotted in Figure 7 and series *D.wav2*, *D.wav4*, *D.wav6*, *D.wav8* and *D.sca10* are plotted in Figure 8.

Since Haar wavelets have been used for the analysis, we can verify the notion in the *MODWT coefficients* section that "wavelet coefficients are associated with changes between two adjacent weighted averages whereas these averages have an effective length of 2^{j-1}". For example, the series of the 4th level wavelet coefficients for T has been calculated as follows:

$$T.wav4_t = 1/16 \sum_{m=0}^{7} T_{t-m} - 1/16 \sum_{m=8}^{15} T_{t-m}, \quad \text{for} \quad t = 15,...,N-1.$$

Therefore, we can clearly see that this series is indeed associated with changes (the minus sign) between two adjacent averages (smoothers), whereas these averages have an effective length of $2^{4-1} = 8$. For the ease of the further discussion we present the individual levels of wavelet coefficients and the corresponding frequency ranges and time scales associated with these levels in Table 1.

Table 1

Wavelet coefficients of different levels and the corresponding frequency and time scale ranges.

Level of wavelet coefficients	Corresponding frequency range	Changes between averages which are calculated on the time scale of
1	$2^{-2} < f \leq 2^{-1}$	2^{1-1} day = 1 day
2	$2^{-3} < f \leq 2^{-2}$	2 days
3	$2^{-4} < f \leq 2^{-3}$	4 days
4	$2^{-5} < f \leq 2^{-4}$	8 days ≈ 1 week
5	$2^{-6} < f \leq 2^{-5}$	16 days
6	$2^{-7} < f \leq 2^{-6}$	32 days ≈ 1 month
7	$2^{-8} < f \leq 2^{-7}$	64 days
8	$2^{-9} < f \leq 2^{-8}$, contains the frequency year $^{-1}$	128 days
9	$2^{-10} < f \leq 2^{-9}$	256 days
10	$2^{-11} < f \leq 2^{-10}$	512 days

In our text below, our main interest will be focused on the series of wavelet coefficients for T and D. If the original time series T and D were stationary (i.e. realizations of stationary stochastic processes), then the series of corresponding wavelet coefficients would be stationary too (i.e. realizations of stationary stochastic processes) and their sample means would be close to zero (see also the section *MODWT coefficients*). Indeed, visual inspection of Figure 7 and Figure 8 suggests that the series of wavelet coefficients for T and D are indeed stationary. In Table 2, we give the summary statistics (specifically, sample means and sample variances[4]) for the series of wavelet

4 The sample variances were calculated under the assumption that the mean of the process of wavelet coefficients is zero (see section *MODWT coefficients*).

coefficients for *T* and *D*. Only those coefficients that are not affected by the circularity assumption have been used in the calculation.

The sample means of wavelet coefficients of different levels for *T* as well as for *D* are close to zero as might have been expected (if *T* and *D* themselves were stationary). Moreover, for *D,* the sample means of wavelet coefficients are slightly negative and tend to more negative values for higher levels. This suggests (due to the way the coefficients were calculated) a slight downward trend in *D*. This is in agreement with the visual inspection of Figure 1 and with the series of scaling coefficients of the 10th level for *D* which is plotted in Figure 8 – these scaling coefficients capture (due to their definition and properties) long-term movements in the original series *D*.

It can be shown (see e.g. Percival & Walden, 2002; or Bašta, 2010) that the sample variances of wavelet coefficients are related to the contribution of the respective frequency range (or time scale) – associated with these coefficients – to the sample variance of *T* (or *D*). Informally, we may say that the higher the sample variance of wavelet coefficients, the higher the contribution of the respective frequency range to the sample variance of *T* (or *D*). Therefore, it can be intuitively seen that whereas the dynamics of *T* has a strong seasonal component (i.e. the sample variance of the series of the 8th level wavelet coefficients is large), the dynamics of *D* has a weaker seasonal component and a strong high-frequency component (i.e. the sample variance of the series of the 1st level wavelet coefficients is large).

Figure 7

The Haar MODWT wavelet coefficients of (from top to bottom) the 2nd, 4th, 6th and 8th levels, and the scaling coefficients of the 10th level for *T*. The solid vertical lines mark the position of the last coefficient affected by the circularity assumption.

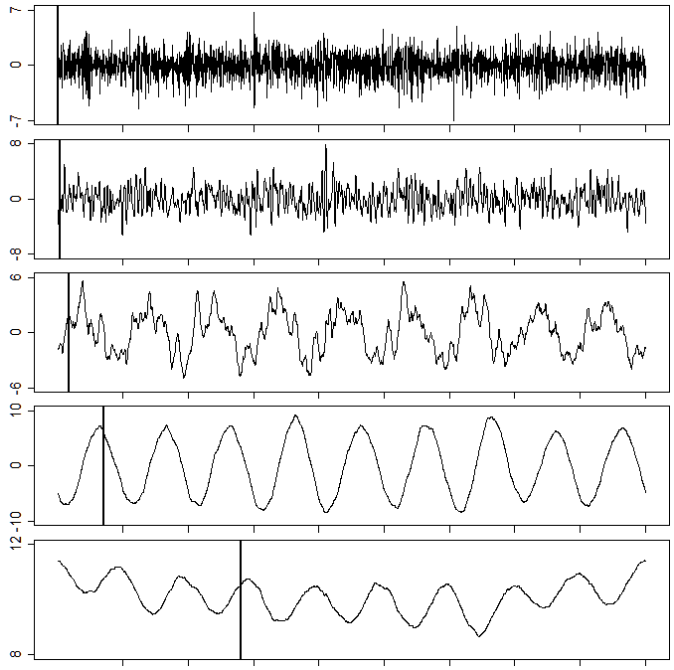

It is also interesting to note that the series of wavelet coefficients of high levels for *T* and *D* (see e.g. level 6 of wavelet coefficients in Figure 7 and Figure 8) are not sufficiently smooth as they would be if they had been obtained by the linear filtration with a true *ideal* linear filter for the respective frequency band. This is due to the fact that the Haar filter $\{h_{j,t}\}$ is only a rough approximation to the ideal filter of the nominal pass band $[2^{-(j+1)}, 2^{-j}]$ (see also Figure 6). It can be shown that if other families (e.g., Daubechies-4, Daubechies-8, etc.) of wavelets had been used instead of Haar wavelets, a better approximation to ideal filters might have been achieved and the resultant wavelet coefficients of higher levels would be a bit smoother. However, the purpose of our text is not to achieve the best approximations to ideal filters, but to have results that can be interpreted easily at the end. Due to the simple structure of Haar filters, these filters are preferred in our case.

Figure 8

The Haar MODWT wavelet coefficients of (from top to bottom) the 2nd, 4th, 6th and 8th levels, and the scaling coefficients of the 10th level for *D*. The solid vertical lines mark the position of the last coefficient affected by the circularity assumption.

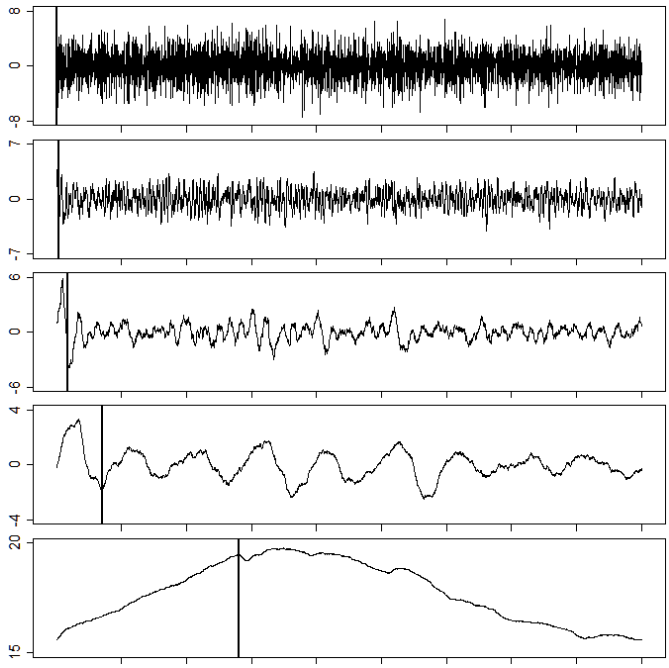

Table 2

The summary statistics for the Haar MODWT wavelet coefficients for *T* and *D*. Only coefficients not affected by the circularity assumption have been used. In the calculation of the sample variance, the process mean was supposed to be equal to zero.

Level of wavelet coefficients	Sample mean of wavelet coefficients for T	Sample variance of wavelet coefficients for T (assuming a zero mean process)	Sample mean of wavelet coefficients for D	Sample variance of wavelet coefficients for D (assuming a zero mean process)
1	-9×10^{-4}	1.46	-2×10^{-3}	8.95
2	-2×10^{-3}	2.19	-4×10^{-3}	4.54
3	-3×10^{-3}	2.72	-7×10^{-3}	2.44
4	1×10^{-3}	2.82	-1×10^{-2}	1.37
5	9×10^{-3}	3.07	-3×10^{-2}	0.88
6	7×10^{-3}	5.09	-4×10^{-2}	0.76
7	3×10^{-2}	13.67	-5×10^{-2}	0.62
8	4×10^{-2}	27.16	-8×10^{-2}	0.79
9	-4×10^{-2}	5.08	-0.14	0.31
10	0.12	2.38	-0.41	0.45

4. The relationship between wavelet coefficients

The seasonal dynamics

The relationship between the wavelet coefficients for *T* and the wavelet coefficients for *D* may reveal interesting characteristics of the relationship between temperature and the number of deaths. For example, the seasonal pattern of the relationship between *T* and *D* might be easily captured within the relationship of the wavelet coefficients of the 8th level, which corresponds to seasonal variations (see Table 1). Thus, in Figure 9 we present a scatterplot of *D.wav8* against *T.wav8* smoothed by the lowess smoother. One can clearly see that the seasonal changes in the temperature (i.e. changes caused by changing seasons of the year) are negatively correlated with the seasonal changes in the number of deaths (i.e. changes in the number of deaths exhibiting roughly a one-year period).

Such a result is in agreement with the V-shaped curve of Figure 2, which slightly suggested that winter (i.e. low) temperatures are accompanied on average by a higher number of deaths and spring and summer (i.e. high) temperatures are accompanied on average by a lower number of deaths. However, this seasonal relationship was overlaid by the dynamics of other frequency bands and was thus poorly seen in Figure 2. However, the plot of Figure 9 captures *only* the seasonal motions themselves with other frequency bands omitted. Therefore, the seasonal relationship which was poorly seen in Figure 2 is clearly seen in Figure 9.

Figure 9

The scatterplot of *D.wav8* against *T.wav8* (smoothed by the lowess smoother). Only coefficients not affected by the circularity assumption have been used.

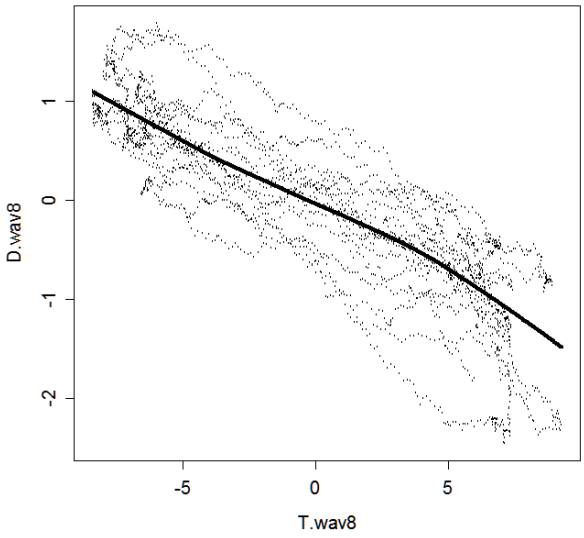

Relationship on intermediate time scales

The seasonal relationship captured between *T* and *D* is well-known (see also the section *Introduction and data*). Above, we have detected it with the use of the 8th level wavelet coefficients. Abrupt changes in temperature and the number of deaths might be explored with the use of 1st level wavelet coefficients. We will not pursue this goal in our text. On the other hand, we have decided to study the relationship between *T* and *D* on low and intermediate levels of wavelet coefficients, specifically on levels 2, 3, 4 and 5.

In Figure 10 we represent the matrix of scatterplots of *D.wavX* against *T.wavX* for $X = 2, ...,5$. Each of these plots might be informally interpreted as the relationship between *T* and *D* for the respective frequency band (e.g. frequency band $[2^{-5}, 2^{-4}]$ in case of $X = 4$). The 2nd, 3rd and 5th level wavelet coefficients do not suggest any interesting relationships. On the other hand, the situation seems to be *slightly* different for the 4th level wavelet coefficients. More specifically, as suggested by the lowess smoother, there seems to be a *slight* positive linear relationship between *D.wav4* and *T.wav4* for almost the whole sample range of *T.wav4* – i.e. an increase in *T.wav4* causes an increase in *T.wav4*. This relationship is broken (as suggested by the lowess smoother) only for large values of *T.wav4*, where an increase in *T.wav4* causes a decrease in *D.wav4* (however, the significance of this break is likely to be low as there are only a few data points corresponding to large values of *T.wav4*).

On the other hand, this break in the relationship between *T.wav4* and *D.wav4* occurring for large values of *T.wav4* may be suggestive of another variable being possibly important in explaining the variation of *D.wav4*. A possible choice of this variable

is the season of the year. In our analysis, December, January and February represent *winter*; March, April, May represent *spring*; June, July and August represent *summer*; and September, October and November represent *autumn*. In Figure 11, the scatterplot of *D.wav4* against *T.wav4* is presented separately for winter, spring, summer and autumn. The estimates of the slopes of the linear relationship (obtained by ordinary least squares[5]) are given in Table 3. These results suggest the relationship might be of practical importance for summer.

Figure 10

The matrix of scatterplots of *D.wavX* against *T.wavX* for *X* = 2, 3, 4, 5 (smoothed by the lowess smoother). Only coefficients not affected by the circularity assumption have been used.

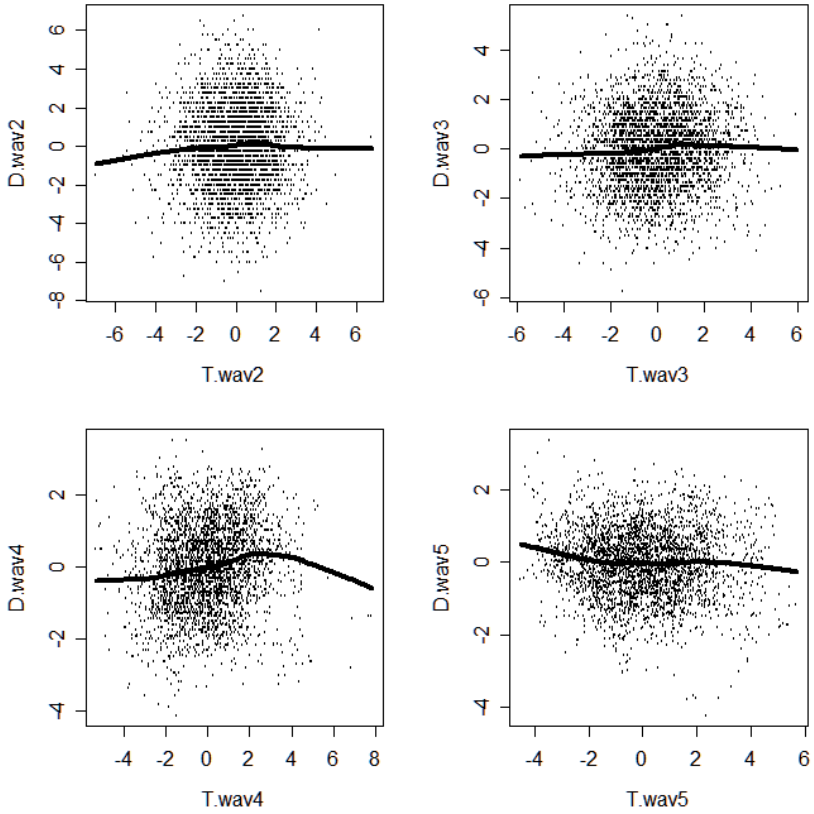

5 See also the text below for the adjustment for the correlation in errors.

Figure 11 also suggests that the relationship between *D.wav4* against *T.wav4* might be slightly nonlinear (at least for some seasons). Therefore, we will assess whether an increase in *T.wav4* is more likely to cause an increase in *D.wav4* (when compared with the decrease of *T.wav4*). We group the coefficients *T.wav4* into two categories.

The dichotomization of *T.wav4* at 0 is as follows: The first category for *T.wav4* corresponds to nonpositive values of *T.wav4* (i.e. $T.wav4 \leq 0$). The second category for *T.wav4* corresponds to positive values of *T.wav4* (i.e. $T.wav4 > 0$). Similarly, we group the coefficients of *D.wav4* into two categories. The dichotomization of *D.wav4* at 0 is as follows: The first category for *D.wav4* corresponds to nonpositive values of *D.wav4* (i.e. $D.wav4 \leq 0$). The second category for *D.wav4* corresponds to positive values of *D.wav4* (i.e. $D.wav4 > 0$). Such a dichotomization is very practical from the point of view of interpretation of the categories. The respective counts for the categories are given in Table 5 for each season. The ratio of odds (*OR.4*) in favor of *D.wav4* being positive under the condition that *T.wav4* is positive to the odds in favor of *D.wav4* being positive under the condition that *T.wav4* is nonpositive is defined as

$$OR.4 \equiv \frac{P(D.wav4 > 0 \mid T.wav4 > 0) \Big/ P(D.wav4 \leq 0 \mid T.wav4 > 0)}{P(D.wav4 > 0 \mid T.wav4 \leq 0) \Big/ \mathrm{P}(D.wav4 \leq 0 \mid T.wav4 \leq 0)} ,$$

where $P(A|B)$ is the conditional probability of A, given B. The estimates of *OR.4* for different seasons are given in Table 4. The results support the idea of a relationship between *T.wav4* and *D.wav4* for summer, which was already found above.

The 95% confidence intervals for the slopes of linear regression and for *OR.4* in Table 3 and Table 4 are much wider than what the original data might imply[6]. The reason for this is the fact that the errors in the regressions are *correlated*. This stems from the fact that adjacent wavelet coefficients are highly correlated because they are in fact overlapping moving averages and thus use common data for their calculation. To correct for this fact, we have assumed in the calculation of confidence intervals that the series of jth level wavelet coefficients decorrelates only after the length 2^j (see also Percival & Walden, 2002). This approach is conservative, in the sense that it is very likely that it produces wider 95% confidence intervals than they truly are.

6 Also the significance of the *t* test and Wald tests might be different from what the original data imply.

Figure 11

The scatterplot of *D.wav4* against *T.wav4* grouped by the seasons of the year (smoothed with the lowess smoother). Only coefficients not affected by the circularity assumption have been used.

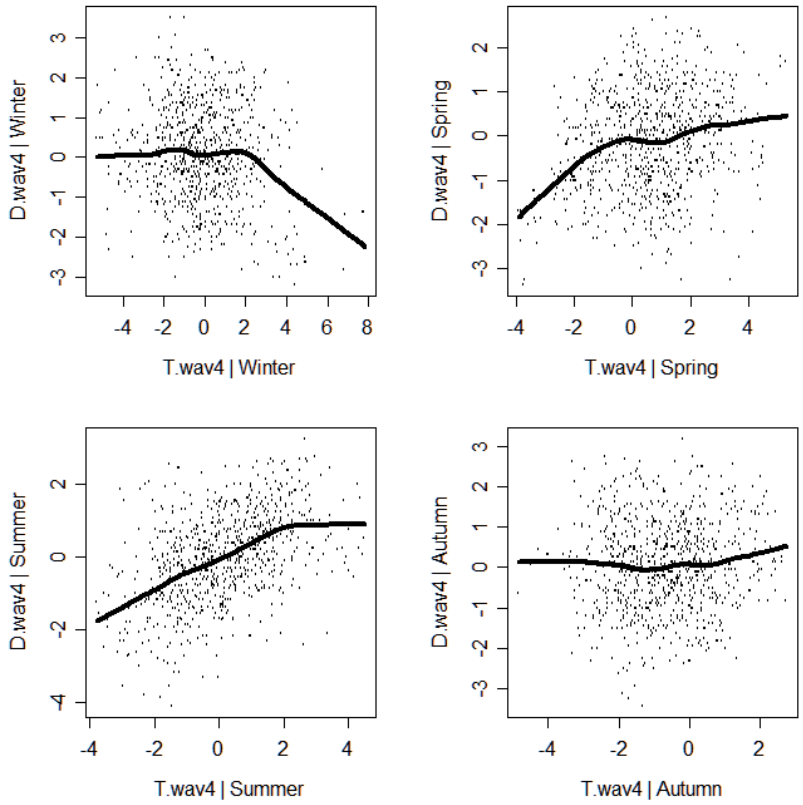

Table 3

The linear regression of *D.wav4* against *T.wav4* for different seasons of the year. The estimates of the slope of the regression and 95% confidence intervals are provided. The calculation of the confidence intervals adjusts for the correlation of wavelet coefficients (see the text for details). The significance of the slope was tested with the *t* test (again adjustment for the correlation was applied), and the results are denoted as follows: - not significant at 5 %, * significant at 5 %. The diagnostics of the residuals was carried out involving the tests of homoscedasticity, autocorrelation (after having adjusted for it at first) and normality and visual inspection of residual plots. An OK is to denote that no significant violations of the assumptions (i.e. homoscedasticity of the error term, no autocorrelation in errors, and normality of errors) have been found.

	Season	WINTER	SPRING	SUMMER	AUTUMN
Linear regression	*est(slope)*	-0.08	0.15	0.37	0.04
	95% CI, slope	(-0.25, 0.10)	(-0.03, 0.33)	(0.17, 0.56)	(-0.19, 0.27)
	t test	–	–	*	–
	diagn. control	*OK*	*OK*	*OK*	*OK*

Table 4

The estimation of odds OR.4. Point estimates as well as 95% confidence intervals are presented. The calculation of the confidence intervals adjusts for the correlation of wavelet coefficients (see the text for details). To test whether OR.4 is significantly different from unity, the Wald test was utilized (again adjustment for the correlation was applied). The results are denoted as: - not significant at 5 %, * significant at 5 %.

	Season	WINTER	SPRING	SUMMER	AUTUMN
Odds estimation	*est(OR.4)*	0.99	2.03	4.22	1.23
	95% CI, OR.4	(0.32 , 3.01)	(0.61, 6.74)	(1.32, 13.50)	(0.38, 4.01)
	Wald test	–	–	*	–

Table 5

Counts in individual categories for the four seasons of the year.

WINTER	Cat. 1: *T.wav4* ≤ 0	Cat. 2: *T.wav4* > 0	Sum
Cat. 1: *D.wav4* ≤ 0	212	179	**391**
Cat. 2: *D.wav4* > 0	222	185	**407**
Sum	**434**	**364**	**798**
SPRING	Cat. 1: *T.wav4* ≤ 0	Cat. 2: *T.wav4* > 0	Sum
Cat. 1: *D.wav4* ≤ 0	176	268	**444**
Cat. 2: *D.wav4* > 0	94	290	**384**
Sum	**270**	**558**	**828**
SUMMER	Cat. 1: *T.wav4* ≤ 0	Cat. 2: *T.wav4* > 0	Sum
Cat. 1: *D.wav4* ≤ 0	276	149	**425**
Cat. 2: *D.wav4* > 0	123	280	**403**
Sum	**399**	**429**	**828**
AUTUMN	Cat. 1: *T.wav4* ≤ 0	Cat. 2: *T.wav4* > 0	Sum
Cat. 1: *D.wav4* ≤ 0	285	119	**404**
Cat. 2: *D.wav4* > 0	274	141	**415**
Sum	**559**	**260**	**819**

The temporal changes

Wavelets are suitable for exploring different time scales as well as for studying temporal patterns in the data. We may easily assess whether the slopes of the linear regression of *D.wav4* on *T.wav4* for summer were stable during the years 2000 to 2008. In Figure 12, we present the scatterplots of *D.wav4* against *T.wav4* for the summers of years 2000 to 2008 together with the least squares lines.

To assess whether the slopes for individual years are significantly different from each other, we may use the model

$$D.wav4_t = \beta_0 + \beta_1 \times T.wav4_t + \sum_{i=1}^{8} \gamma_i \times (T.wav4_t \times Y_{i,t}) + \varepsilon_t,$$

where $Y_{i,t}$ is a dummy variable defined as

$$Y_{i,t} = \begin{cases} 1, & \text{for year } 2000+i \\ 0 & \text{otherwise} \end{cases}$$

and where β_0, β_1 and γ_i are parameters and ε_t is an error term. The null hypothesis of $\gamma_1 = \gamma_2 = \ldots = \gamma_8 = 0$ cannot be rejected (at the 5% significance level) – again the correlation of wavelet coefficients was taken into account. We may conclude that we are not able to reject the null hypothesis of stable slopes of the linear regression of *D.wav4* on *T.wav4*.

Figure 12

The scatterplot of *D.wav4* against *T.wav4* for summers of different years (together with the least squares line). Only coefficients not affected by the circularity assumption have been used.

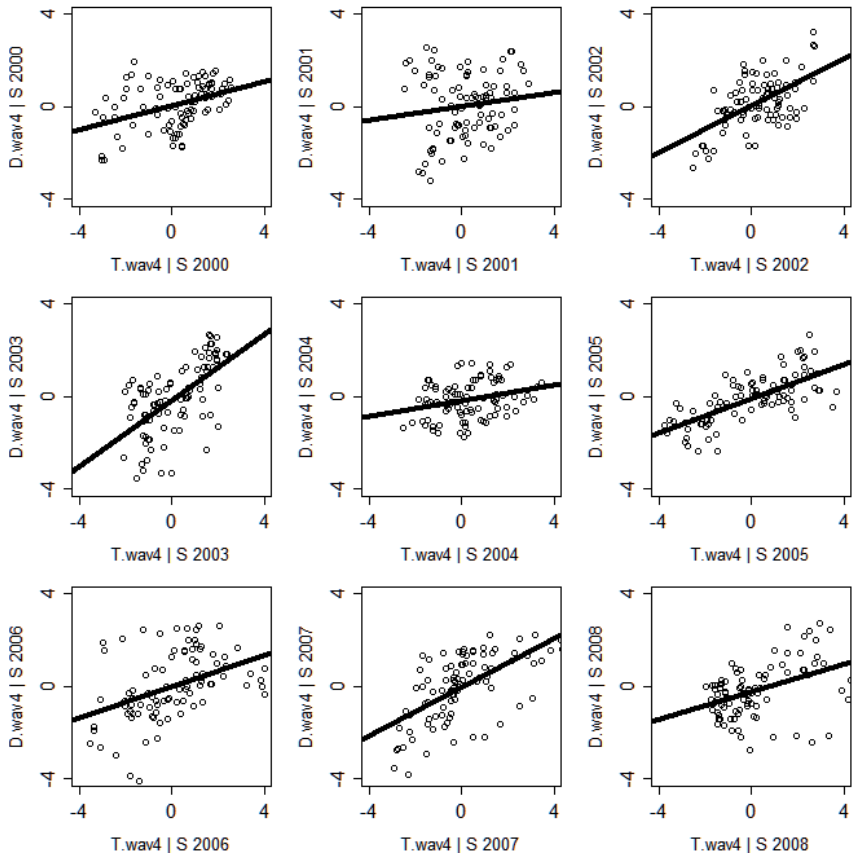

5. Discussion and conclusion

In this paper, we have used the Haar maximum overlap discrete wavelet transform to explore the relationship between the ambient temperature and the numbers of deaths due to cardiovascular diseases on different time scales. At first, we verified the seasonal antiphase relationship between temperature and the numbers of deaths. Afterwards, we studied the dynamics on other time scales. Our results suggest that a positive linear relationship is present between the 4th level of the wavelet coefficients of the time series of temperature and the 4th level of the wavelet coefficients of the time series of the numbers of deaths.

To interpret the results, we have to realize that Haar wavelet coefficients of level 4 are in fact differences of two adjacent non-overlapping moving averages, whereas both the moving averages are a one-half multiple of the simple moving average of 8 days. As 8 days are almost one week, we may informally interpret the results in the following manner: Changes in the weekly average temperature during summer are accompanied by the changes in the weekly average numbers of deaths due to cardiovascular diseases. More specifically, a one-degree-Celsius increase in the weekly average temperature in summer is accompanied on average by a 0.37 increase in the number of deaths due to cardiovascular diseases. We have also shown that no significant temporal evolution in the slope of the linear relationship is present in the data set.

Moreover, the odds in favor of an increase in the weekly average number of deaths due to cardiovascular diseases given an increase in the weekly average temperature were found to be 4.22 times higher than the odds in favor of an increase in the weekly average number of deaths due to cardiovascular diseases given a decrease in the weekly average temperature.

It might be also interesting to pinpoint the exact time scale at which the relationship is the strongest, since in our study the chosen time scales were the powers of 2 (see Table 1). Therefore, we could have easily missed the true time scale which occurs somewhere in between the powers of 2.

Even though the nominal confidence coefficients used in the data analysis have been 95 %, it is clear from the way the data have been analyzed (i.e. several levels of wavelet coefficients have been explored, the data were separated into subgroups, the "promising" group was selected for further analysis) that the true confidence coefficient is "a bit" lower. Therefore, we may conclude that this paper suggests that an interesting relationship may exist between temperature and the number of deaths. Future verifications of the relationship on independent data sets (from other countries, temporal epochs) are necessary and so is the discussion on the plausibility of this relationship from the medical and climatological view.

References

BAŠTA, M. 2010. Waveletová transformace a její aplikace při analýze ekonomických a finančních časových řad [Doktorská dizertační práce]. Praha : VŠE, Fakulta informatiky a statistiky, 2010.

BAŠTA, M.; ARLT, J.; ARLTOVÁ, M.; HELMAN, K. 2010. Continuous Wavelet Transform and the Annual Cycle in Temperature and the Number of Deaths. In *COMPSTAT 2010.* Paris : CNAM; INRIA, 2010, s. 761.

CLEVELAND, W. 1979. Robust Locally Weighted Regression and Smoothing Scatterplots. *Journal of the American Statistical Association*. 1979, vol. 74, s. 829.

DÍAZ, J.; GARCÍA, R.; LÓPEZ, C.; LINARES, C.; TOBÍAS, A.; PRIETO, L. 2005. Mortality Impact of Extreme Winter Temperatures. *International Journal of Biometeorology*. 2005, vol. 49, s. 179.

GENCAY, R.; SELCUK, F.; WHITCHER, B. 2002. *An Introduction to Wavelets and Other Filtering Methods in Finance and Economics*. Academic Press, 2002. ISBN 9780122796708.

GRIZE, L.; HUSS, A.; THOMMEN, O.; SCHINDLER, C.; BRAUN-FAHRLANDER, C. 2005. Heat Wave 2003 and Mortality in Switzerland. *Swiss Medical Weekly*. 2005, vol. 135, s. 200.

HYUNEN, M.; MARTENS, P.; SCHRAM, D.; WEIJENBERG, M.; KUNST, A. 2001. The Impact of Heat Waves and Cold Spells on Mortality Rates in the Dutch Population. *Environmental Health Perspectives*. 2001, vol. 105, s. 463.

KEATINGE, W.; DONALDSON, G. 1995. Cardiovascular Mortality in Winter. *Arctic Medical Research*. 1995, vol. 54, s. 16.

LARSEN, U. 1990. The Effects of Monthly Temperature Fluctuations on Mortality in the United States from 1921 to 1985. *International Journal of Biometeorology*. 1990, vol. 34, s. 136.

LASCHEWSKI, G.; JENDRITZKY, G. 2002. Effects of the Thermal Environment on Human Health: An Investigation of 30 Years of Daily Mortality Data from SW Germany. *Climate Research*. 2002, vol. 21, s. 91.

PERCIVAL, D.; WALDEN, A. 2002. *Wavelet Methods for Time Series Analysis*. Reprint. Cambridge : Cambridge University Press, 2002. ISBN 9780521640687.

ROONEY, C.; McMICHAEL, A.; KOVATS, R.; COLEMAN, M. 1998. Excess Mortality in England and Wales, and in Greater London, During the 1995 Heatwave. *Journal of Epidemiology and Community Health*. 1998, vol. 52, s. 482.

VIDAKOVIC, B. 1999. *Statistical Modeling by Wavelets*. Wiley-Interscience, 1999. ISBN 9780471293651.

THE MODWT ANALYSIS OF THE RELATIONSHIP BETWEEN MORTALITY AND AMBIENT TEMPERATURE FOR PRAGUE, CZECH REPUBLIC

Abstract: Weather conditions influence the health of humans. Changing weather patterns may also cause considerable increase or decrease in the number of deaths. In this paper, we use daily data for Prague, Czech Republic, and the maximum overlap discrete wavelet transform to explore the time scale patterns in the relationship between the average ambient temperature and the number of deaths due to cardiovascular diseases. We summarize several well-known facts, give a short introduction to the maximum overlap discrete wavelet transform and study the relationship between several pairs of wavelet coefficients of various levels for the temperature time series and the number of deaths. The results are suggestive of a positive linear relationship between respective wavelet coefficients of the 4th level during summer. More specifically, we have estimated that a one-degree-Celsius increase in the weekly average temperature during summer is accompanied by an increase in the weekly average number of deaths by 0.37 on average. The odds in favor of an increase in the weekly average number of deaths during summer have been estimated to be 4.22 times higher if an increase in the weekly average temperature occurs when compared to the situation when a decrease in the weekly average temperature occurs. Further research might be desirable to verify and interpret the results.

Keywords: MODWT, demography, time series, mortality, temperature

JEL Classification: C10, I12